Pierre Auger Project Note: GAP-99-XYZ

HiRes Note: MM-DD-1999

Analysis of Time Variant Molecular Atmosphere for the Purpose of Air Fluorescence Measurements

Georgianna Martin, John A.J. Matthews
[1] *New Mexico Center for Particle Physics*
University of New Mexico
Albuquerque, NM 87131, USA

October 11, 1999

Abstract

The next generation air fluorescence experiments studying cosmic rays near 10^{20}eV require significantly better atmospheric monitoring than the original Fly's Eye experiment. In this paper we study the time variant vertical profile of the atmosphere. For this study we use the 00-hour radiosonde data from the Salt Lake City(SLC) and Reno(REN) airports. The relevance of the time and altitude variation on the molecular component of the transmission correction is discussed.

1 Introduction:

The HiRes and future Auger fluorescence detectors use the atmosphere as their readout system. Therefore, understanding the atmosphere is of the utmost importance. There are three types of atmospheric variations: clouds, aerosols and time dependences in the molecular atmosphere. In this analysis we concentrate on the molecular component of the atmosphere and on their effect on the transmission corrections to the air fluorescence data.

The amount of transmitted light, I, seen by the detector is directly proportional to the amount of scatterers the source light encounters in the atmosphere between the source and the fluorescence detector:

$$I \sim I_0 \cdot T^m \cdot T^a$$

where:

I = Intensity of light 'seen' at the detector

I_o = Intensity of source

T^m = Transmission molecular component

T^a = Transmission aerosol component

The molecular component of the transmission correction is potentially well known. By comparison the aerosol component is poorly known. To minimize the overall transmission uncertainty it is prudent to have the molecular uncertainty $\ll$ the aerosol uncertainty.

2 Transmission Correction(Rayleigh Scattering),T^m:

For this analysis we assume a completely molecular atmosphere. The molecular transmission, T^m, is dependent on the wavelength, λ,of the light signal, and on the direction, θ, and height, Δz, of the light source with respect to the fluorescence zenith and on detector:

$$T^m \equiv T^m(\lambda, \theta, \Delta z) = e^{\int_0^{\Delta z} \frac{\rho(z)dz}{\Lambda^m(\lambda)} \frac{1}{\cos(\theta)}} \quad (1)$$

where: $z = 0$ is set by the altitude of the fluorescence detector, θ is measured from the zenith, and the inverse Rayleigh scattering "cross section", $\Lambda_m(\lambda)$, is:

$$\Lambda^m(\lambda) = 2970 \cdot (\frac{\lambda}{400nm})^4 \ \ gm/cm^2$$

The integral of the atmospheric density is to a good approximation:

$$\int_0^{\Delta z} \rho(z)\, dz \ \ = \ \ \frac{\delta P(\Delta z) mbar \cdot 10}{g(m/s)} \ \ \ (in\ gm/cm^2) \tag{2}$$

where $\delta P(\Delta z)$, is the pressure difference between the pressure at ground height, taken as 1500m, and the pressure at the source height, Δz. The fractional uncertainty in T^m is then:

$$\frac{\Delta T^m}{T^m} \ \ \approx \ \ (\frac{1}{\cos(\theta)}) \ \cdot \ \frac{\Delta(\delta P(\Delta z)) \cdot 10}{g \cdot \Lambda^m(\lambda)} \tag{3}$$

where $\Delta(\delta P)$ (in mbar) is the uncertainty in the pressure difference between the real time pressure profile and the proposed model.

If we require

$$\frac{\Delta T^m}{T^m} \leq n(\%)$$

then at $\lambda =$ 350nm (near the center of the fluorescence telescope acceptance) the uncertainty in the pressure difference, $\Delta(\delta P)$, should be less than:

$$\Delta(\delta P) \leq n(\%) \cdot 17\ mbar \cdot cos(\theta) \tag{4}$$

Alternatively, the quantity we are truly interested in, the error, can be represented by the following equation:

$$n(\%) \sim \frac{1}{(17\ mbar) \cdot cos(\theta)} \cdot \Delta(\delta P) \tag{5}$$

3 Radiosonde Data

A study of the time variation of the (molecular) atmosphere is made possible thanks to data from frequent radiosonde measurements carried out by the weather service.

In particular,data used in this analysis were collected by weather balloons sent up from the weather stations at the Salt Lake City and Reno airports. These balloons carry atmospheric monitoring equipment up to heights as high as 100,000m. The atmospheric data are constantly transmitted during the balloon's $\sim$ 90min flight. The balloon then bursts and the equipment deploys a parachute and falls back to the Earth. The radiosonde data banks were accessed through the use of the RAOB web site[1]. The balloons are flown at 00:00 and 12:00. Due to the nature of night time observing by fluorescence detectors, the 00:00, or midnight, data were used in this analysis. The data used in this analysis included data from 1996, 1997 and 1998.

4 Analysis of Molecular Atmospheric Models

For this analysis the SLC radiosonde data were taken to represent the *actual pressure* profile of the atmosphere. Then various models for the atmosphere were compared to the SLC data. The pressure difference between SLC data and the model is then the error $\Delta(\delta P)$

$$\Delta(\delta P) \equiv (\delta P)_{SLC \quad radiosonde} - (\delta P)_{model} \tag{6}$$

The fractional uncertainties in the molecular transmission corrections are proportional to $\Delta(\delta P)$, see Eqn. 3: thus this study provides a straight forward estimate of the transmission correction uncertainties. For a given fluorescence experiment, it is of interest to know which atmospheric model (or models) meet the experimental constraint:*e.g.* $\frac{\Delta T^m}{t^m} \sim 2\%$ (or less)?

The $\Delta(\delta p)$ data depend on height,Δz (and of course time). The fluorescence telescopes record light over a range of angles, θ, and from showers over a range of (horizontal) distances, $R_\perp$. These are (trivially) related:

$$\Delta z = \frac{R_\perp}{tan(\theta)} \tag{7}$$

For this study we choose two different horizontal distances from the detector: $R_\perp =$ 20 km and 40 km, typical maximum shower distances for Auger and HiRes experiments respectively, and three viewing angles: $\theta = 85°, 80° and 75°$, typical of*ring 1* mirrors in hires; see table 1.

Table 1: Source heights, Δz, corresponding to typical shower horizontal distances in Auger (20km) and HiRes (40km) and for typical fluorescence detector viewing angles from the zenith.

$R_\perp$	θ	Δz
20km	85^o	1800m
	80^o	3500m
	75^o	5400m
40km	85^o	3500m
	80^o	7100m
	75^o	10700m

In this study we focus on how the error, Eqn 5, varies *versus* viewing angle,θ, and viewing distance, $R_\perp$ (or equivalently height, Δz), and as a function of time throughout the year for three different atmospheric models:

- a time independent adiabatic model[2]
- a time dependent adiabatic model
- the pressure profile generated from the Reno radiosonde data.

To show how the actual pressure differences, $\Delta(\delta P)$ (mbar), vary*versus* height (and time), the time independent model results for January 1998 are given in Fig 1a and for July in Fig 1b. These same pressure differences averaged over all of 1998 and given in Fig 2.

4.1 Time Independent Model

For the *time independent model* we use the adiabatic portion of the US Standard Atmosphere[2], to predict the pressure (and temperature) *versus* z. The ground temperature and pressure at sea level are 288.15K and 1013.25mbars respectively. The adiabatic portion of the US Standard atmospheric model is valid to heights $\leq 11,000m$. This is sufficient for the analysis, as most fluorescence measurements come from below 11,000m.

$$T(z) \;=\; 288.15 \;-\; 6.5 \cdot \frac{z}{1000} \tag{8}$$

$$P(z) \quad = \quad 1013.25 \cdot (\frac{T(z)}{288.15})^{5.255877} \tag{9}$$

The results fir 1998 are shown in Fig 3a & b and indicate that showers at horizontal ranges of 20km and 40km would have rather large fractional uncertainty in transmission errors, are least during some times of the year. Thus while the time independent model satisfies the $\sim$ 2% range in the winter months, the summer months are clearly not consistent with the $\sim$ 2% range.

4.2 Time Dependent Model

For the *time dependent model* the daily ground temperature and pressure (at midnight) are the starting points for the adiabatic atmosphere:

$$T(\Delta z) \quad = \quad daily\ ground\ T \ - \ 6.5 \cdot \frac{\Delta z}{1000} \tag{10}$$

$$P(\Delta z) \quad = \quad daily\ ground\ P \cdot (\frac{T(\Delta z)}{daily\ ground\ T})^{5.255877} \tag{11}$$

where, Δz = source height - ground height(1500m).

The results are presented in Fig 4a & b(1996), Fig 5a & b(1997) and Fig 6a & b(1998). The fractional in the transmission correction us significantly reduced in comparison to the time independent model. Furthermore the fractional uncertainty for showers at a horizontal distance of 20km is consistently $< 2\%$. For showers at 40km the fractional uncertainty $\sim$ 2%.

4.3 Reno Radiosonde Model

For the *radiosonde model* we use the radiosonde profile from one site (*e.g.* Reno) to provide the atmosphere (model) for a second site (*e.g.* Salt Lake City). However, fluorescence experiments are not located at an airport. If the precision of the radiosonde pressure profile is called for, the question becomes what is the error involved in being at some distance from the actual radiosonde site. By using the radiosonde data from the Reno airport as a model for the Salt Lake City data, we can test the stability of the pressure profile across the western desert. In Fig 7a & b the fractional uncertainty between SLC and Reno is within the guidelines of the $\sim$ 2% error requirement for both the short range, 20km, and long range,40km, showers. The comparison between the 1997 data, Fig. 7a & b, and the 1998 data, Fig. 8a & b, shows no obvious yearly trend

(or trends). Furthermore there does not appear to be any systematic fluctuations in the data set. The random fluctuations suggest that the fractional transmission corrections based on using radiosonde data will be $\sim 1\%$ or less.

5 Summary

From this analysis we make several observations. The time independent model, Sect. 4.1, is insufficient for making fluorescence detector atmospheric transmission corrections at the few percent level. In contrast the time dependent model, Sect. 4.2, is probably sufficient for both Auger and HiRes experiments. For experiments striving to measure showers at distances of 40km or more, the pressure profile generated from the local airport radiosonde data will provide the most accurate model for the molecular atmosphere. The choice of atmospheric models will depend on the accessibility of an airport in proximity to the experiment *versus* the expense and operation of temperature and pressure measurement equipment. The accessibility of the radiosonde data, http://roab.noaa.fsl.gov/, will allow experiments simple access to radiosonde data for their calibration files. If an airport is not within a acceptable distance, the adiabatic model, combined with local ground temperature and pressure measurements, will result in an uncertainty $\sim 2\%$.

6 References

[1] RAOB web site for radiosonde data: http://raob.fsl.noaa.gov/

[2] US standard Atmosphere (1976), CRC Handbook of Chemistry and Physics, **72**, **14**-12 (1991)

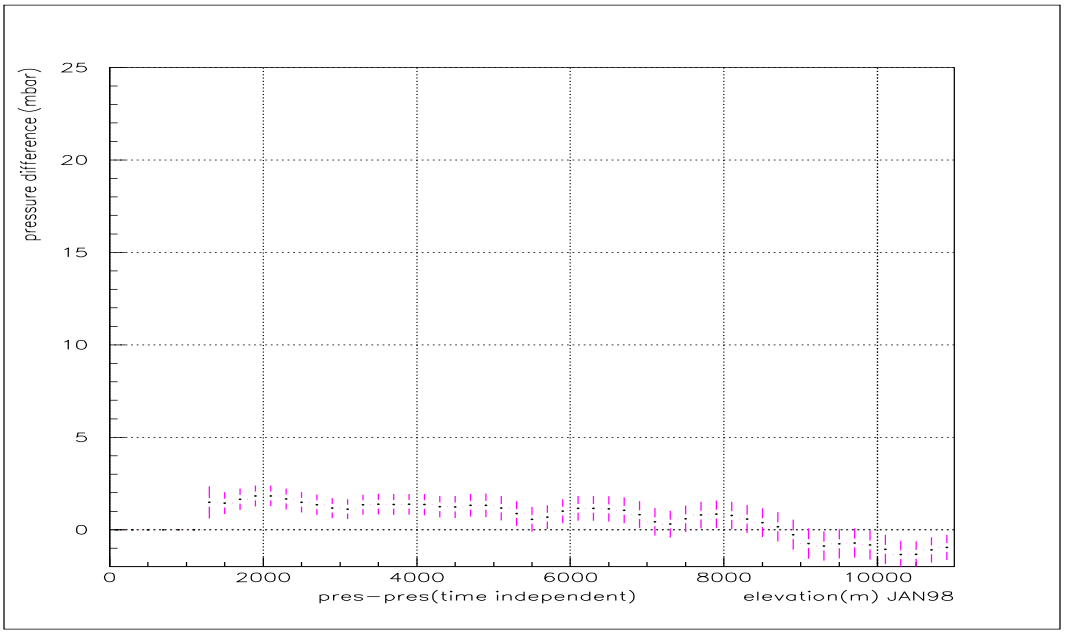

Fig. 1a: Pressure difference,as in Fig 2., as a function of height above sea level for the month of January, 1998. The pressure difference $\sim 1-2$mbars suggest that the model estimates the pressure in the winter months with a small error(Eqn 5).

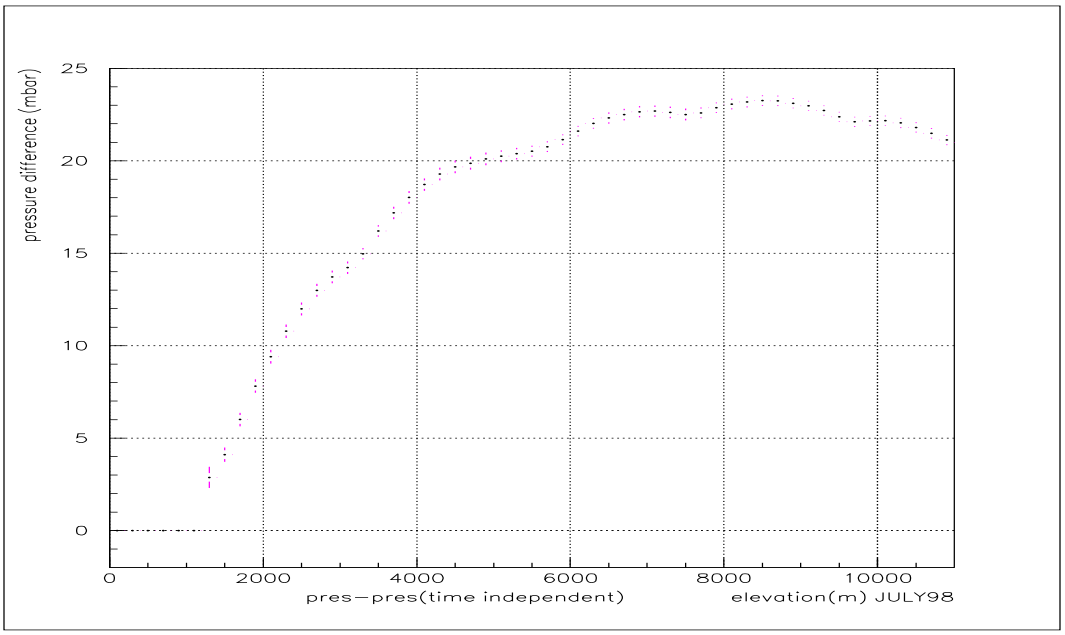

Fig. 1b: Pressure difference,as in Fig 2., as a function of height above sea level for the month of July, 1998. The pressure difference $\sim 2-25$mbars suggest that the model estimates the pressure in the summer months with a large error(Eqn 5).

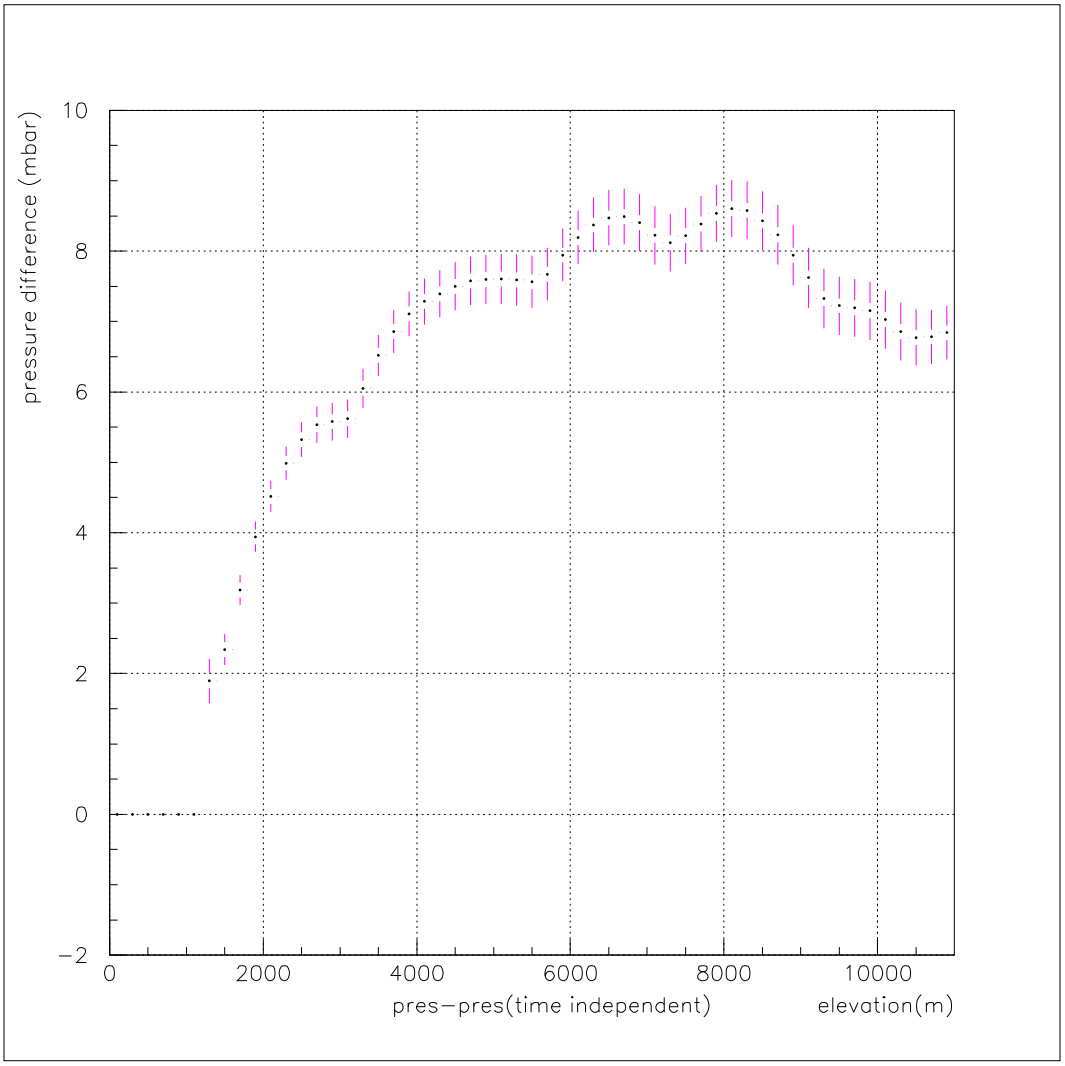

Fig. 2: Pressure difference, $\delta P_{SLC} - \delta P_{time\ indep}$, as a function of height above sea level over the span of one year(1998).

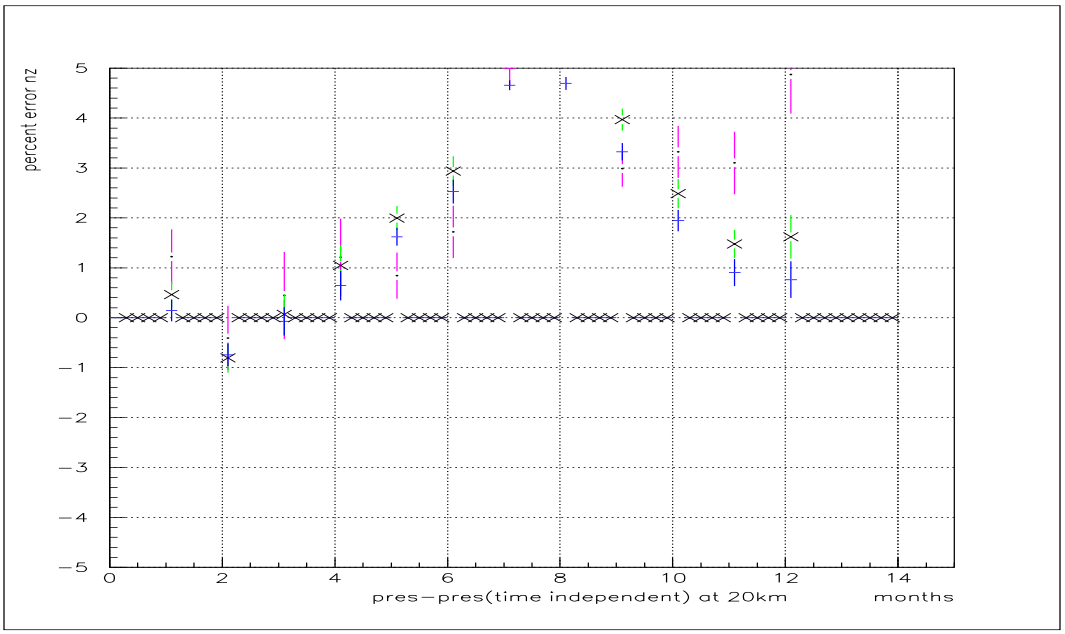

Fig. 3a: Fractional uncertainty, $\frac{\Delta T^m}{T^m}$, (Eqn. 5) for the*time independent* model at a radius of 20km, over the span of one year (1998) for three angles of elevation: $\theta = (85^o = \cdot, 80^o = X, 75^o = +)$

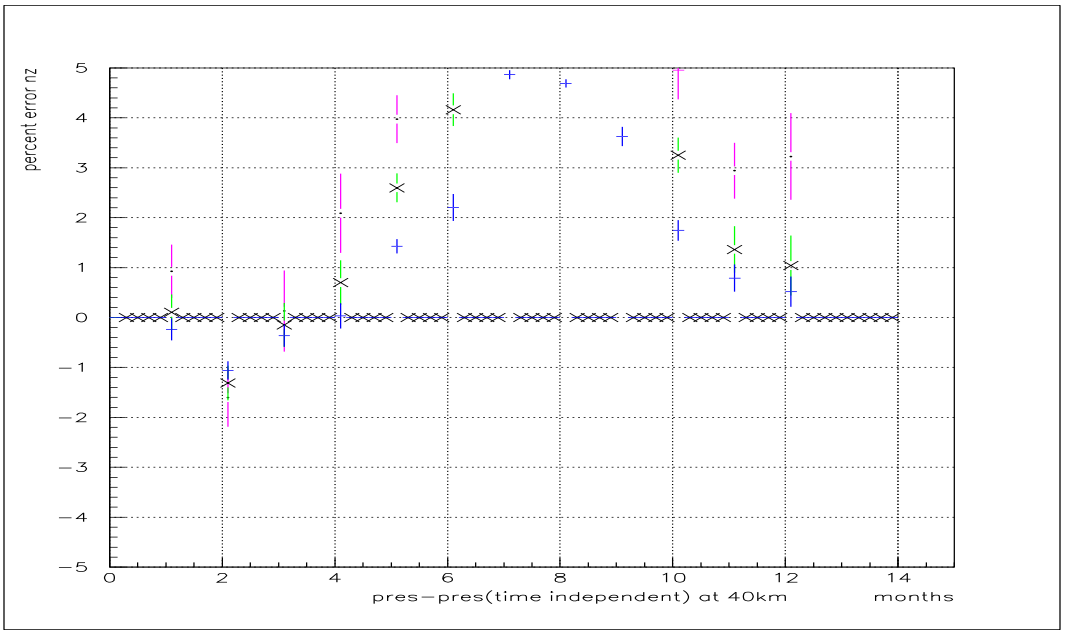

Fig. 3b: Fractional uncertainty, $\frac{\Delta T^m}{T^m}$, (Eqn. 5) for the*time independent* model at a radius of 40km, over the span of one year (1998) for three angles of elevation: $\theta = (85^o = \cdot, 80^o = X, 75^o = +)$

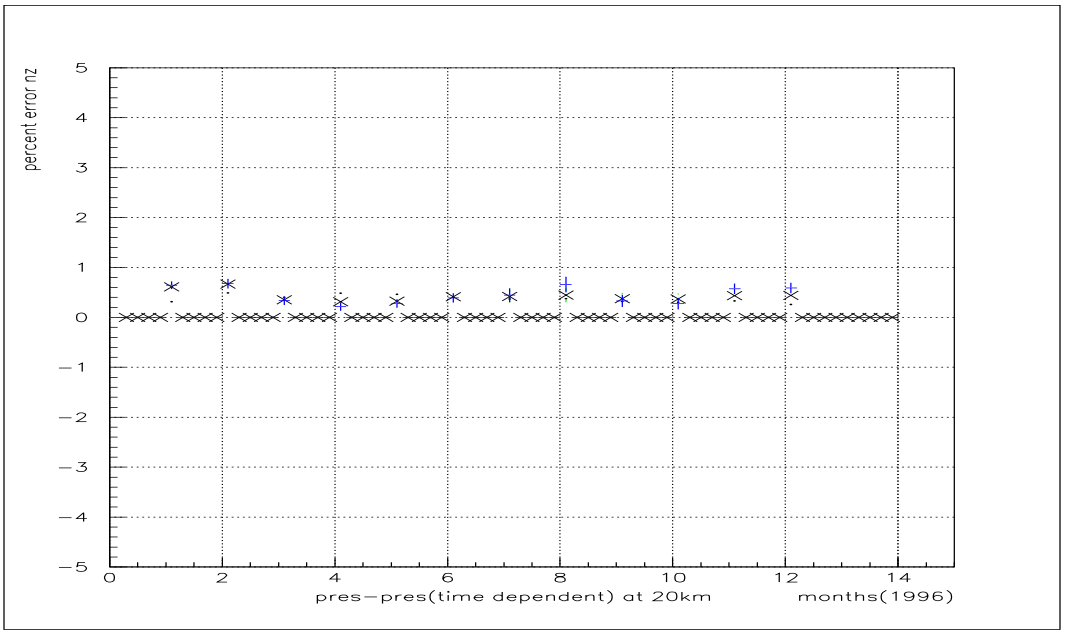

Fig. 4a: Fractional uncertainty (Eqn. 5) in the $\Delta T^m/T^m$ for the*time dependent* model at a radius of 20km, over the span of one year (1996)) for three angles of elevation: $\theta = (85^o = \cdot, 80^o = X, 75^o = +)$.

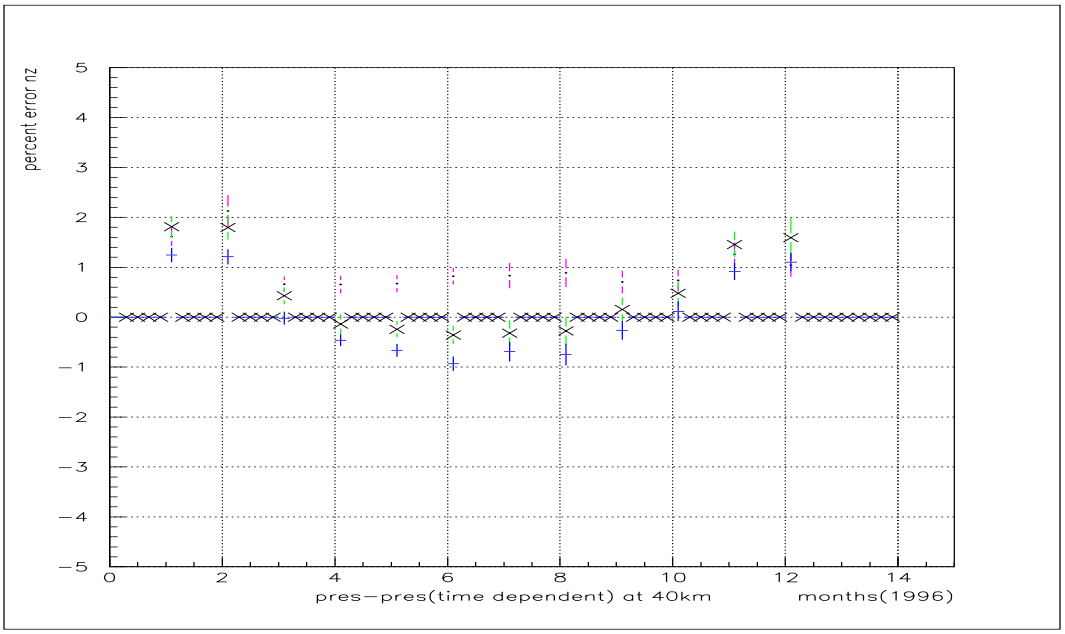

Fig. 4b: Fractional uncertainty (Eqn. 5) in the $\Delta T^m/T^m$ for the*time dependent* model at a radius of 40km, over the span of one year (1996)) for three angles of elevation: $\theta = (85^o = \cdot, 80^o = X, 75^o = +)$.

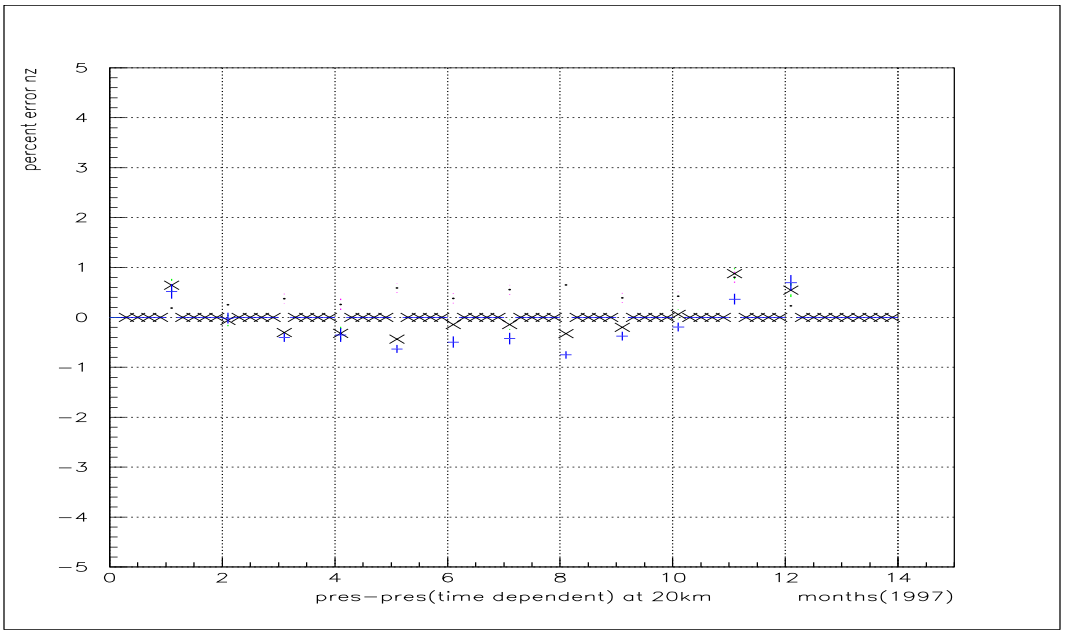

Fig. 5a: Fractional uncertainty (Eqn. 5) in the $\Delta T^m/T^m$ for the*time dependent* model at a radius of 20km, over the span of one year (1997)) for three angles of elevation: $\theta = (85^o = \cdot, 80^o = X, 75^o = +)$.

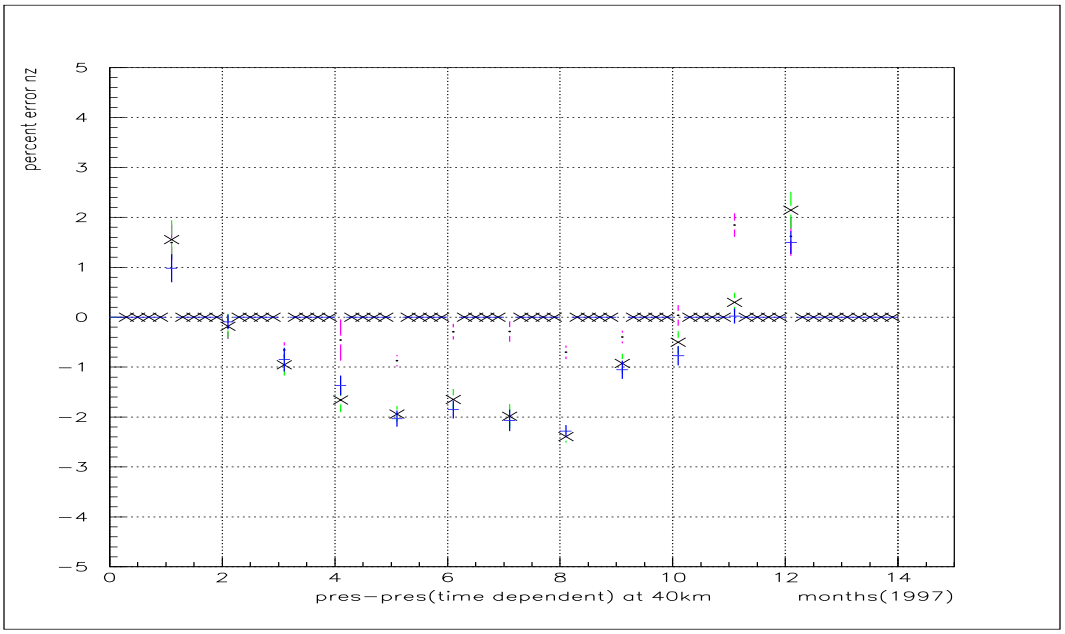

Fig. 5b: Fractional uncertainty (Eqn. 5) in the $\Delta T^m/T^m$ for the*time dependent* model at a radius of 40km, over the span of one year (1997)) for three angles of elevation: $\theta = (85^o = \cdot, 80^o = X, 75^o = +)$.

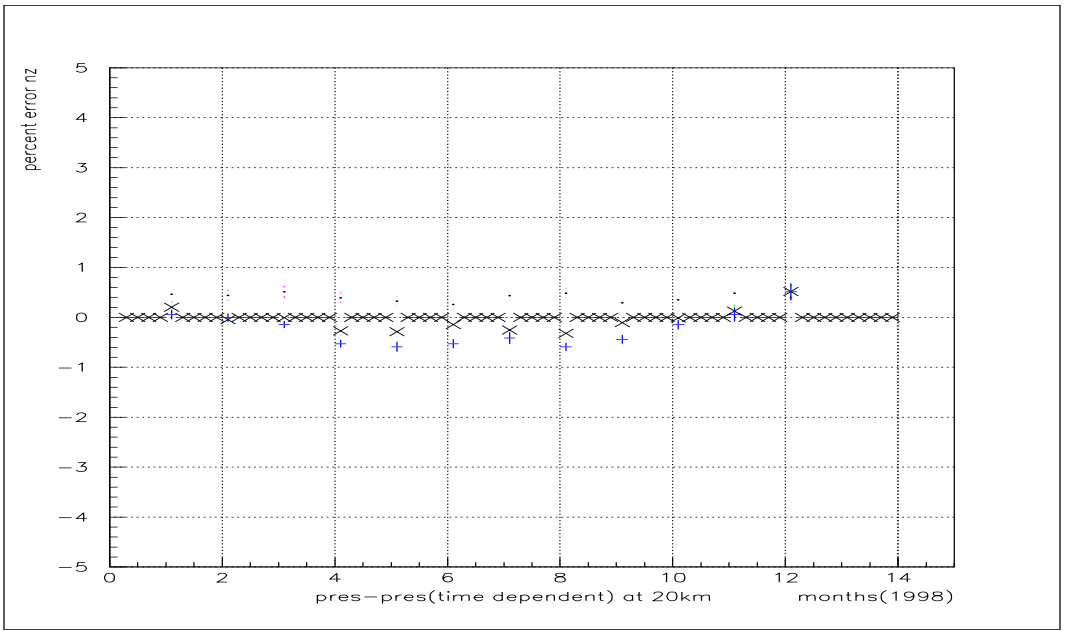

Fig. 6a: Fractional uncertainty (Eqn. 5) in the $\Delta T^m/T^m$ for the*time dependent* model at a radius of 20km, over the span of one year (1998)) for three angles of elevation: $\theta = (85^o = \cdot, 80^o = X, 75^o = +)$.

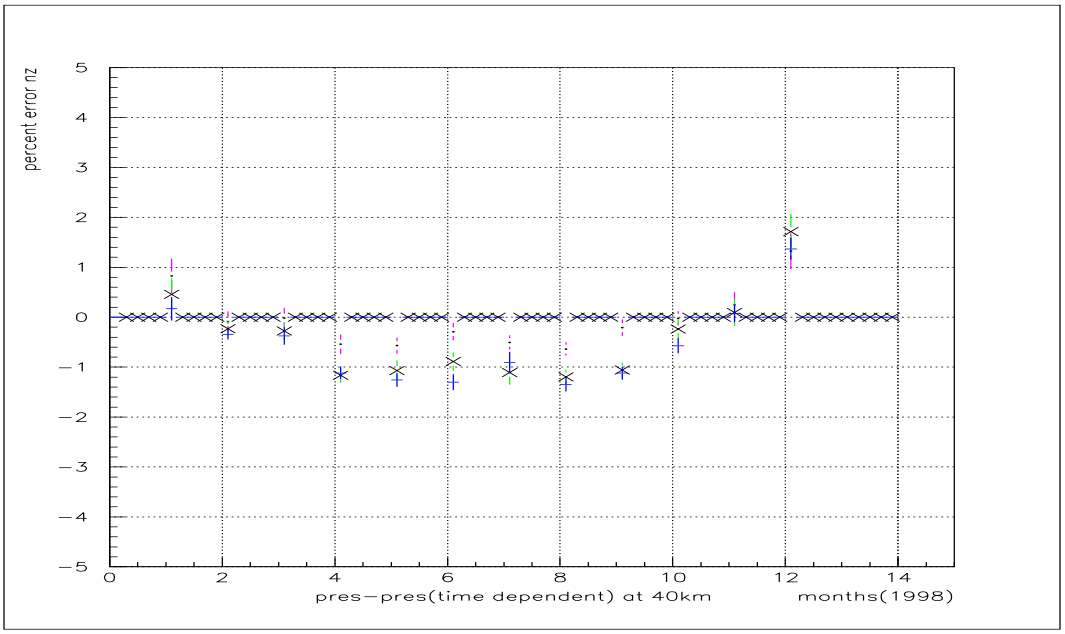

Fig. 6b: Fractional uncertainty (Eqn. 5) in the $\Delta T^m/T^m$ for the*time dependent* model at a radius of 40km, over the span of one year (1998)) for three angles of elevation: $\theta = (85^o = \cdot, 80^o = X, 75^o = +)$.

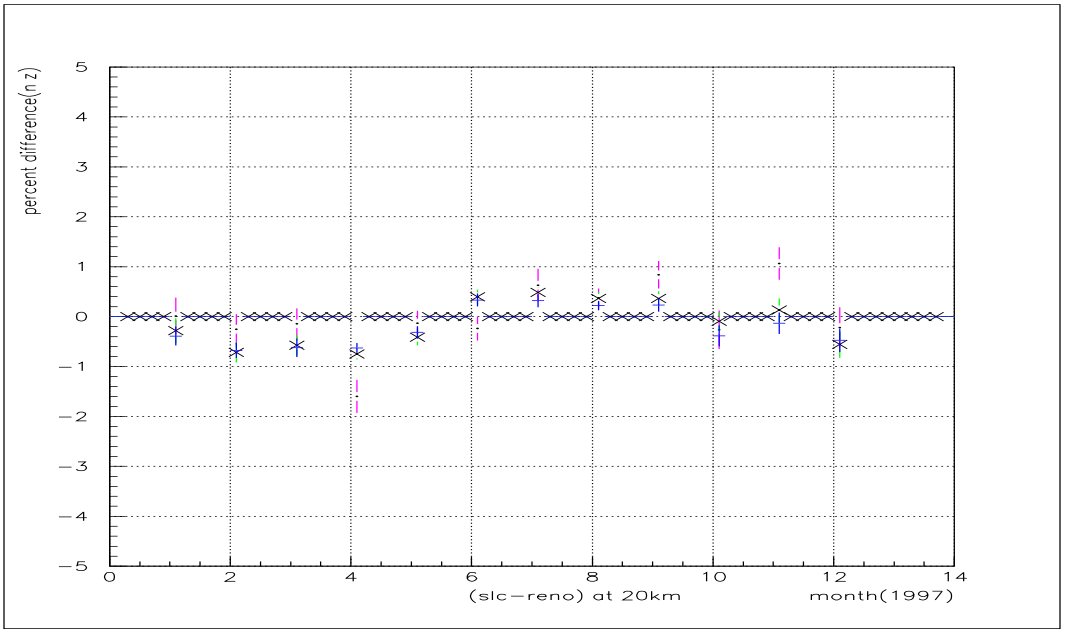

Fig. 7a: Fractional uncertainty (Eqn. 5) in the $\Delta T^m/T^m$ for the*Reno radiosonde model* model at a radius of 20km, over the span of one year (1997)) for three angles of elevation:

$\theta = (85^o = \cdot, 80^o = X, 75^o = +)$.

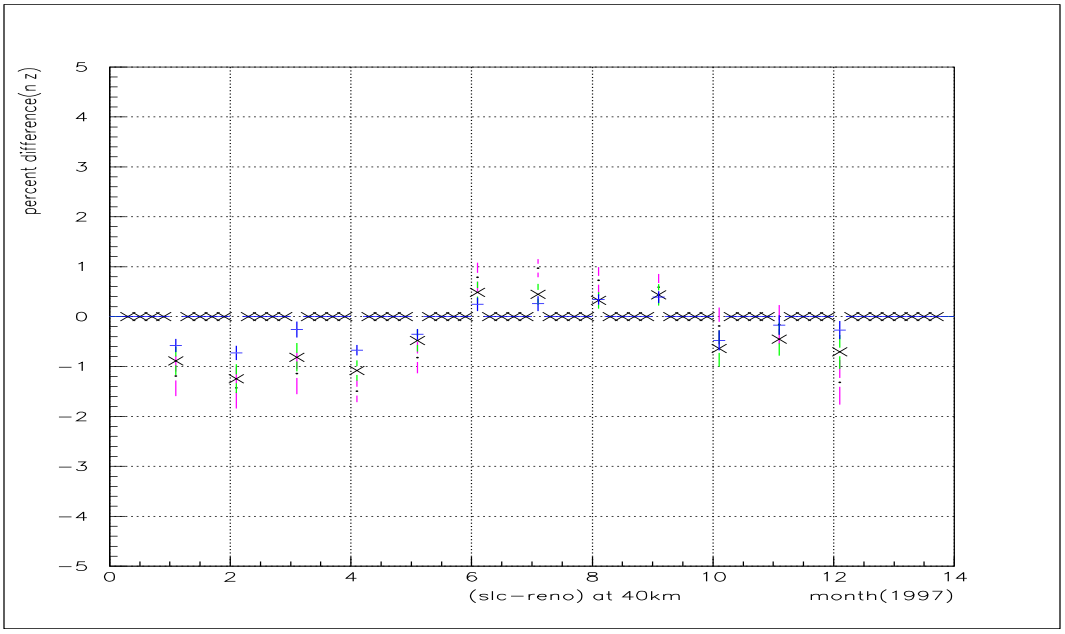

Fig. 7b: Fractional uncertainty (Eqn. 5) in the $\Delta T^m/T^m$ for the*Reno radiosonde model* model at a radius of 40km, over the span of one year (1997)) for three angles of elevation:

$\theta = (85^o = \cdot, 80^o = X, 75^o = +)$.

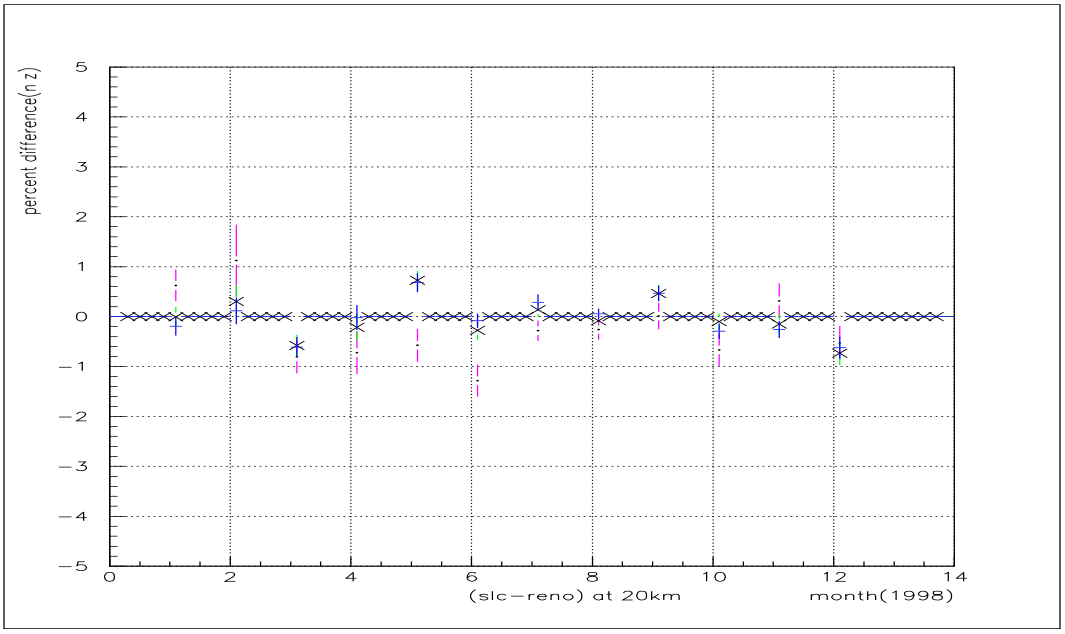

Fig. 8a: Fractional uncertainty (Eqn. 5) in the $\Delta T^m/T^m$ for the*Reno radiosonde model* model at a radius of 20km, over the span of one year (1998)) for three angles of elevation:

$\theta = (85^o = \cdot, 80^o = X, 75^o = +)$.

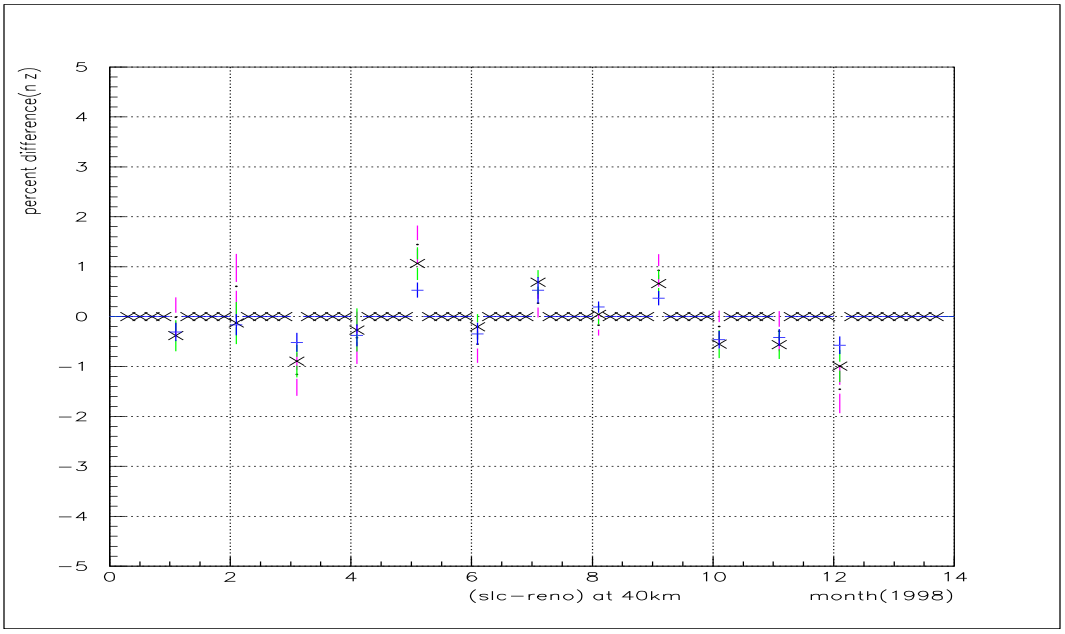

Fig. 8b: Fractional uncertainty (Eqn. 5) in the $\Delta T^m/T^m$ for the*Reno radiosonde model* model at a radius of 40km, over the span of one year (1998)) for three angles of elevation:

$\theta = (85^o = \cdot, 80^o = X, 75^o = +)$.